Available online www.jsaer.com

***Journal of Scientific and Engineering Research*, 2022, 9(4):7-16**

Research Article

ISSN: 2394-2630
CODEN(USA): JSERBR

Recent GNSS-Based Estimates of Vertical Land Movements in the Nile Delta, Egypt Over 2012-2019

Hoda F. Mohamed, Gomaa M. Dawod*

Survey Research Institute, National Water Research Center, Giza, Egypt
* dawod_gomaa@yahoo.com, ORCID = 0000-0002-4426-8231

Abstract This paper aims to determine reliable and up-to-date estimates of the vertical land movements in the Nile delta region based on high-precision datasets of Global Navigation Satellite Systems (GNSS) observations covering the period 2012-2019. Repeated data, every 6 months, of 23 GNSS stations have been collected, processed, and analyzed using the Precise Point Positioning (PPP) GNSS technique. Geographic Information Systems (GIS) tools have been applied to model the 3D spatial variations of crustal deformation across the Nile delta. Based on the available data and the accomplished results, it is concluded that the vertical land movements within the study area range from subsidence equals -5.5 mm/year to uplift equals 4.2 mm/year, with an overall average of -0.08 mm/year. Additionally, it has been found that Port Said, Kafr El-Zaiat, and Tanta cities suffer from high land subsidence rates while Cairo, Belbis, Fakous and Burrllus cities are subjected to high trend of uplift. Regarding the Sea Level Rise (SLR) in the Nile delta, it is estimated that taking land subsidence into account, the absolute SRL at Alexandria and Port Said equal 6.0 mm/year and 7.6 mm/year respectively. Such findings should be highly considered in the development plans of those cities, particularly for huge infrastructures. Furthermore, the current research recommends the continuation of GNSS-based monitoring of such phenomena over a longer time.

Keywords GNSS, Sea Level Rise, Land Subsidence, PPP, GIS, Nile Delta

Introduction

Monitoring vertical land movements, subsidence or uplift, comprise an essential geodetic theme to explain the geodynamics of the planet Earth over a specific spatial extent. Land subsidence, among other environmental hazards, causes several physical and human dangerous impacts to the public worldwide, particularly in low-land areas and coastal regions. Basically, land subsidence could be identified as the down displacement of the land surface relative to a definite reference surface, such as Mean Sea Level (MSL) or an ellipsoid. This phenomenon could be attributed to both natural and human-induced reasons such as geology structures, soil characteristics, groundwater withdrawal and other factors [1]. In the last few decades, the geodetic community has paid attention to precisely monitoring such phenomena. Several techniques and datasets have been utilized in monitoring land subsidence, particularly the Global Navigation Satellite Systems (GNSS) [2], the Interferometric Synthetic Aperture Radar (InSAR) [3], satellite altimetry and tide gauges data [4], and levelling data [5]. A combination of several observing techniques would be more efficient in monitoring land subsidence. Many research studies have been conducted in several countries for the monitoring and risk assessment of land subsidence, e.g. in Indonesia [6], Turkey [7], and the Czech Republic [8].

The Nile delta, as other rivers' deltas, is typically subjected to land subsidence. Additionally, it is subjected to several other environmental and human challenges such as coastal erosion, land-use changes, water quality determination, sea level rise, soil degradation, groundwater pollution, and shoreline retreat [9]. Ground

subsidence and sea level rise are the most environmental hazards that affect the Nile delta region. Generally, the rate of land subsidence over the entire Nile delta region varies from 2 to 9 mm/year [10]. AbouAly et al [11] have utilized GNSS datasets over 2013-2015 over the Nile delta and Northern part of Egypt and found that land subsidence in the delta range between mm/year 2.5 and 10 mm/year. Rateb and Abotalib [12] have utilized Sentinel-1 radar satellite and GNSS data between 2015 and 2019 to investigate land subsidence in the Nile delta region. They reported subsidence rates of 12-20 mm/year in major cities, such as Zagazig and Tanta in the middle of the delta region, and subsidence rates of 3-8 mm/year along the coasts of the delta. Similarly, Saleh and Becker [13] have estimated land subsidence in major cities in the delta as 6.4, 4.0, 4.8, 10.0, 10.3, and 4.9 mm/year for Cairo, Tanta, Mahala, Mansoura, Damietta, and Port Said respectively. On the other hand, the effects of land subsidence include aquifer salinization, infrastructure damage, increased vulnerability to flooding and storm surges, and permanent inundation of low-lying land [14].

Traditionally, the GNSS consist of both the American Global Positioning System (GPS) and its Russian counterpart (GLONASS). Currently, satellites belonging to both the European Galileo system and the Chinese BeDiou system have been visible for tracking worldwide. Therefore, the expression "quad-GNSS" becomes noticeable in geodetic high-precision applications. The Precise Point Positioning (PPP) is the most accurate GNSS processing method nowadays. It provides the accuracy level needed for high-precision crustal deformation and land subsidence monitoring [15]. Due to its accuracy, Rabah et al. [16] have proposed to utilize the PPP method for datum maintenance and updating of the national geodetic networks of Egypt. Recently, the PPP technique has been applied to estimate the tectonic coordinates changes in Egypt [17].

This paper investigates the utilization of GNSS PPP observations in monitoring the land subsidence in the Nile delta region. It aims to determine reliable and up-to-date estimates of land subsidence in the Nile delta region based on high-precision datasets of GNSS observations covering the period 2012-2019.

Study Area and Available Data

The Nile delta, as the study area, extends from longitude 29.7º E to longitude 32.6º E, and from latitude 29.8º N to latitude 31.6º N (Fig. 1). That region extends more than 300 kilometers along the Mediterranean costs from Port Said on the east to Alexandria on the west, and extends almost 200 kilometers perpendicular south to the coastline to Cairo. Thus, its overall area equals approximately 35,000 square kilometers. With more than fifty million people, that delta could be considered as one of the most densely populated areas worldwide. The topography of the study area (Figure 2) ranges from elevation -29 meters to 870 meters, with an average of 31.9 meters. It can be seen from that figure that the dominant elevation is less than 10 meters in the northern and middle parts of the delta. Moreover, it can be realized that the northern region of the delta area has an elevation of less than almost 5 meters. That reality necessitates performing vulnerability analysis studies regarding the sea rise global phenomena and its hazardous impacts on the Nile delta region. However, researchers emphasize the fact that land subsidence in the Nile Delta might be more environmentally hazardous than the sea level rise phenomena [18].

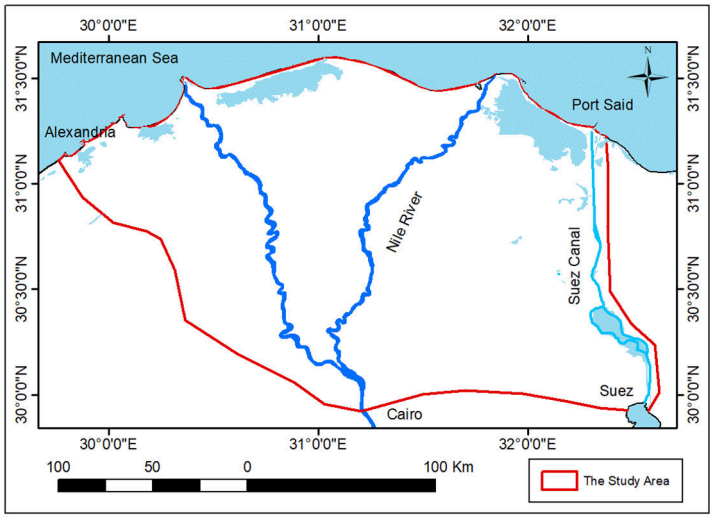

Figure 1: The Study Area

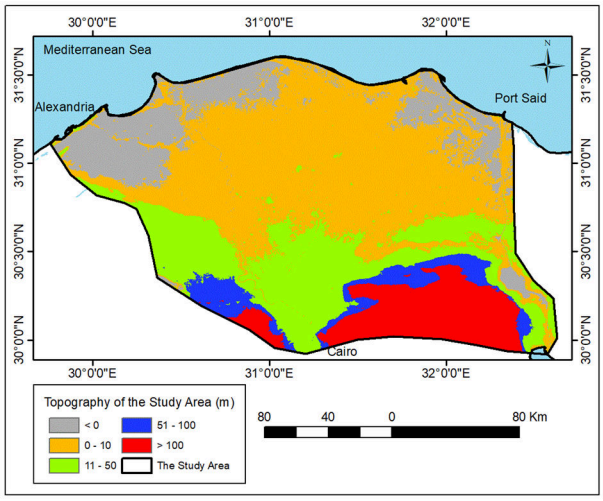

Figure 2: Topography of the Study Area

The utilized dataset (Fig. 3) compresses GNSS raw data of 23 stations of the Virtual Reference Stations (VRS) belonging to the Egyptian Survey Authority (ESA). Forty Continuously Operating Reference Systems (CORS) have been established by ESA in 2010 covering the Nile delta and valley (Fig. 4). Each station is equipped with a dual-frequency GNSS receiver fixed on the top of an ESA building, and every station sends its raw data in real-time to the central ESA office in Cairo. The collected dataset of each utilized session consists of a 24-hour continuous GNSS data in the RINEX (Receiver-INdependent EXchange) format covering the period 2012-2019 with two sessions per year (Table 1). The Trimble Business Center (TBC) v. 5.1 package has been utilized for PPP GNSS data processing [19].

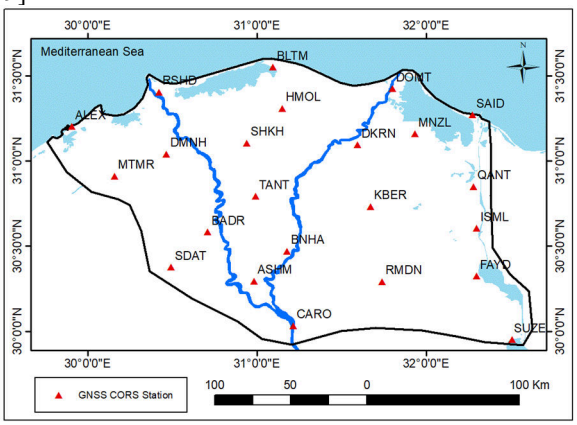

Figure 3: The Utilized GNSS VRS Stations

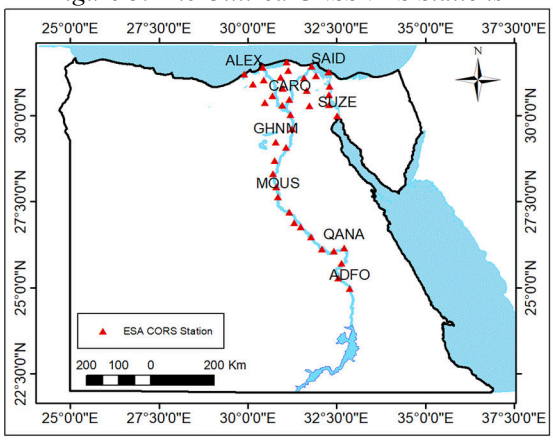

Figure 4: The GNSS VRS Stations in Egypt

Table 1: The Utilized GNSS Raw Data

St. No.	1	2	3	4	5	6	7	8	9	10	11	12	13	14	15	16	17	18	19	20	21	22	23
Year/St.	ALEX	ASHM	BADR	BLTM	BNHA	CARO	DKRN	DMNH	DOMT	FAYD	HMOL	ISML	KBER	MNZL	MTMR	QANT	RMDN	RSHD	SAID	SDAT	SHKH	SUEZ	TANT
2/2012	■	■	■	■	■	■	■	■	■	■	■	■	■	■	■	■	■	■	■	■	■	■	■
1/2013															■								■
7/2013				■									■										■
1/2014				■											■								
7/2014						■							■						■				
1/2015						■							■						■				
7/2015		■	■		■	■			■								■	■					
1/2016	■	■	■			■			■				■			■	■						
7/2016		■	■			■				■			■				■			■			
1/2017	■	■	■		■	■	■	■	■	■		■	■	■	■	■	■	■	■		■		■
7/2017		■	■	■	■	■		■	■		■	■	■	■	■		■		■			■	■
1/2018	■		■	■		■		■	■			■	■	■	■	■	■	■	■				■
7/2018			■	■		■		■				■		■	■		■	■	■	■		■	■
1/2019	■	■	■	■	■	■		■	■		■	■		■	■	■	■		■	■	■	■	■

Methodology

The fundamental idea of the PPP GNSS processing technique comprises the estimation of precise satellites orbits and satellite clock errors based on observations from a high quality global fiducial network, and then the utilization of such information to solve the station parameters of any other sites. The PPP position determination is based on the processing of the following ionosphere-free combination of the un-differenced code and phase observations [20]:

$$P_{Li} = \rho + d_{orb} + c(dT - dt) + d_{ion(L_i)} + d_{trop} + d^{r}_{hd(P_{Li})} - d^{s}_{hd(P_{Li})} + d_{multi(P_{Li})} + d_{noise(P_{Li})} \quad (1)$$

$$\phi_{Li} = \rho + d_{orb} + c(dT - dt) + d_{ion(L_i)} + d_{trop} - \lambda_{Li} N_{Li} + d^{r}_{hd(P_{Li})} - d^{s}_{hd(P_{Li})} + d_{multi(P_{Li})} + d_{noise(P_{Li})} \quad (2)$$

where,

P_{Li} and φ_{Li} represent the pseudorange and carrier phase measurements (in meters) on the frequency L_i respectively,

ρ refers to the geometric distance between the satellite and the receiver,

d_{orb} is satellite orbit error (in meters),

c equals the speed of light in vacuum (in meter/second),

dT and dt denote the clock error of the satellite and the receiver respectively (in seconds),

$d_{ion(Li)}$ is the first-order ionospheric effect on the frequency Li (in meters),

d_{trop} is the troposheric delay (in meters),

$d^{s}_{hd(PLI)}$ and $d^{r}_{hd(PLI)}$ are satellite and receiver hardware delays (in meters) for the Li pseudorange respectively,

$d^{s}_{hd(\varphi LI)}$ and $d^{r}_{hd(\varphi LI)}$ are satellite and receiver hardware delays (in meters) for the Li carrier-phase respectively,

$d_{multi(PLI)}$ and $d_{multi(\varphi LI)}$ represent the multipath errors of the pseudorange and carrier-phase respectively on the frequency L_i (in meters),

$d_{noise(PLI)}$ and $d_{noise(\varphi LI)}$ denote the noise errors of the pseudorange and carrier-phase respectively on the frequency L_i (in meters),

N_{LI} is the ambiguity term on the frequency L_i in cycles, and

λ_{LI} is the wavelength of the frequency L_i (in meters).
The pseudorange and carrier-phase ionospheric-free linear combinations are formed as:

$$P_{if} = \frac{f_1^2 P_1 - f_2^2 P_2}{f_1^2 - f_2^2} \tag{3}$$
$$= \rho + d_{orb} + c(dT - dt) + d^r_{hd(P_{Li})} - d^s_{hd(P_{Li})} + d_{multi(P_{Li})} + d_{noise(P_{Li})}$$

$$\phi_{if} = \frac{f_1^2 \phi_1 - f_2^2 \phi_2}{f_1^2 - f_2^2} \tag{4}$$
$$= \rho + d_{orb} + c(dT - dt) - \lambda_{if} N_{if} + d^r_{hd(\phi_{Li})} - d^s_{hd(\phi_{Li})} + d_{multi(\phi_{Li})} + d_{noise(\phi_{Li})}$$

where,
N_{if} denotes the ionospheric-free ambiguity term (in cycles), and
λ_{if} represents the ionospheric-free wavelength (in meter).
The above formulas show that the unknown parameters to be estimated in PPP include position coordinates, phase ambiguity terms, receiver clock offset, and the troposheric effect. Precise satellite orbits and clock products with the centimeter-level accuracy needed for PPP are now widely available from several global scientific societies. One of such respective organizations is the International GNSS Service (IGS).
It is a matter of reality that the PPP results are, in general, superior to the traditional GNSS data processing. For example, Mohamed [21] has concluded that the accuracy improvements due to using dual-GNSS datasets, i.e. GPS+GLONASS, equal 32%, 35%, and 24% in the X, Y, Z coordinates respectively in Egypt. Generally, applying PPP with observations from quad-GNSS constellation enhances the positional accuracy significantly for multi-frequency or even single-frequency measurements [22].
The processing steps start with importing raw data for the first station, downloading the corresponding precise and clock files from the IGS website, and computing the final coordinates for that station in the first available time epoch. Next, another epoch is similarly processed for that specific station. Having processed all data for this station, their ellipsoidal heights are compared to estimate the vertical movement trend over time. Next, statistical analysis is performed to judge the quality of the accomplished regression results. Iteratively, another station is processed in the same manner until all stations are done. Finally, the Arc GIS software is utilized to develop a 3D surface for the vertical land movements across the study area. Such a processing strategy is depicted in Fig. 5.

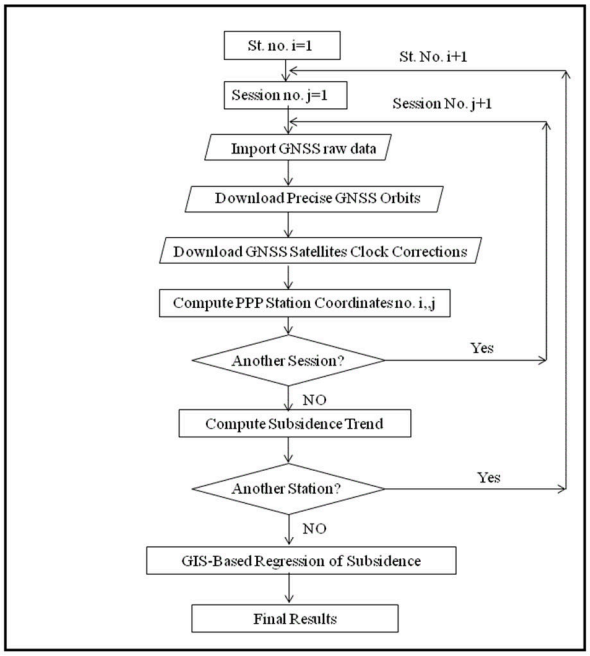

Figure 5: Data Processing Strategy

Moreover, to judge the goodness of the attained linear regression height model at each GNSS station, the coefficient of determination statistical measure, R^2, is applied. It shows the proportion of the variation in the dependant variable that is estimated from the independent variable and it ranges from zero to +1. The higher this value the better the regression model. The coefficient of determination could be estimated as:

$$R^2 = \frac{\sum (\hat{y} - \bar{y})^2}{\sum (y - \bar{y})^2} \quad (5)$$

where,

$\hat{y}$ *and* $\bar{y}$ represent the estimated and average values of the dependant variable respectively.

Processing and Results

Raw GNSS datasets for all available stations have been processed utilizing the PPP approach for each session with respect to the International Terrestrial Reference Frame 2014 (ITRF2014) epoch 2019. Over the utilized GNSS stations, the accomplished findings show that the standard deviation of the X coordinates ranges from 0.011 m to 0.014 m, while it varies from 0.014 m to 0.018 m for the Y coordinates. Similarly, it has been noticed that the standard deviation of the Z coordinates ranges from 0.006 m to 0.009 m. For the geodetic heights, the standard deviation varies between 0.009 m and 0.0011 m. Consequently, it can be concluded that the average precision of the obtained coordinates is at the centimeter level

Furthermore, the variations of height at each station, over the period 2012-2019, have been investigated and a linear regression model has been performed. The coefficient of determination, R^2, in Equation 5 has been computed for the accomplished linear regression model at each station. Table 2 presents the attained findings and reveals important remarks. First, there are 7 stations where R^2 is less than 0.20 which concludes that the linear regression model does not reflect the height variations at those stations. Second, there are four stations with only available 3 observations (GNSS raw data) which shows that the degree of freedom, in the regression modelling, just equals one. Thus, the reliability of the attained regression equations, at these stations, could not be considered trustable. Accordingly, such 11 stations have been neglected and the results of the remaining 12 stations are further investigated (Fig. 6). Table 3 tabulated the reliable results of the regression analysis (R^2 is greater than 0.40) and the attained vertical movements trends in the study area. Thus, it is concluded that the vertical land movements at the twelve reliable GNSS stations within the study area range from subsidence equals -5.5 mm/year to uplift equals 4.2 mm/year, with an overall average of -0.08 mm/year.

Table 2: Statistics of the Attained Regression Models

No	Station	R^2	No. of Observations	No	Station	R^2	No. of Observations
1	ALEX	0.46	9	13	KBER	0.60	6
2	ASHM	0.85	6	14	MNZL	0.51	4
3	BADR	0.004	10	15	MTMR	0.08	5
4	BLTM	0.85	6	16	QANT	0.39	4
5	BNHA	0.01	4	17	RMDN	0.87	5
6	CARO	0.14	7	18	RSHD	0.71	3
7	DKRN	0.88	4	19	SAID	0.55	8
8	DMNH	0.01	7	20	SDAT	0.44	5
9	DOMT	0.88	5	21	SHKH	0.07	3
10	FAYD	0.87	3	22	SUEZ	0.08	4
11	HMOL	0.69	3	23	TANT	0.50	5
12	ISML	0.53	7				

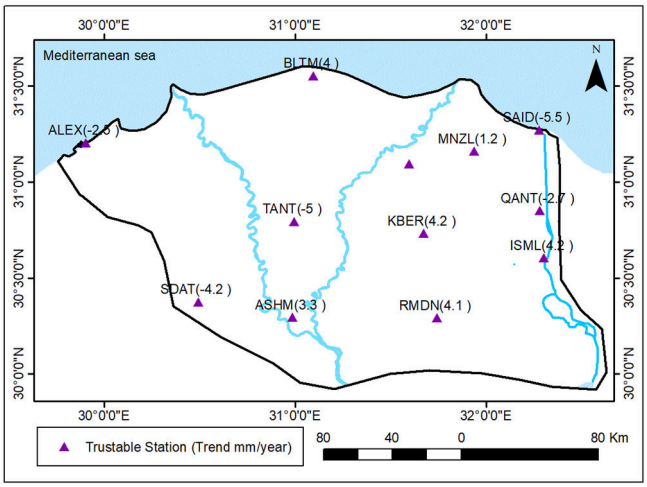

Figure 6: Trustable GNSS Stations and Trends

Table 3: Results of the Attained Vertical Land Movements

No	Station	Regression	Vertical Land Movement Rate (mm/year)
1	ALEX	H = -0.0025 year + 71.935	-2.5
2	ASHM	H = 0.0033 year + 33.144	+3.3
3	BLTM	H = 0.004 year + 22.283	+4.0
4	DKRN	H = -0.0021 year + 42.467	-2.1
5	ISML	H = 0.0042 year + 34.808	+4.2
6	KBER	H = -0.0012 year + 35.579	-1.2
7	MNZL	H = 0.0012 year + 34.593	+1.2
8	QANT	H = -0.0027 year + 39.622	-2.7
9	RMDN	H = 0.0041 year + 141.28	+4.1
10	SAID	H = -0.0055 year + 40.979	-5.7
11	SDAT	H = -0.0042 year + 80.095	-4.2
12	TANT	H = -0.005 year + 51.013	-5.0

Next, the Arc GIS 10 software has been utilized to construct a spatial 3D model of vertical land movements over the Nile delta region (Figure 7). From such a model, it can be concluded that the land motion range from -5.49 mm/year to +4.66 mm/.year, with an average of +0.32 mm/year. That spatial model could be applied to interpolate the vertical land movement annual rate at any location within the study area. Hence, it is quite important in engineering projects in general and particularly for water resources management applications. The attained findings are generally compatible with those of other studies such as Rateb et al. [12] (2020), Saleh et al. [13] (2019), and AbouAly et al. [11] (2021a).

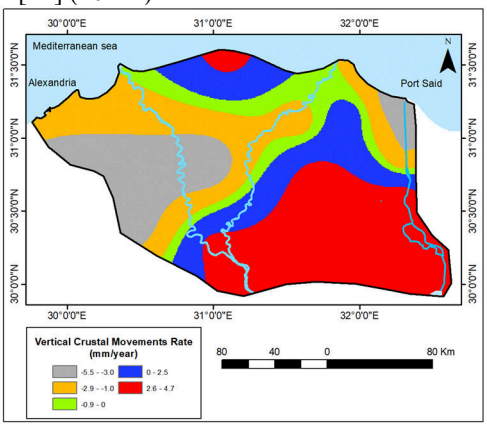

Figure 7: Vertical Land Movements in the Nile Delta over 2012-2019

Next, the main cities in the Nile delta region have been plotted on the attained 3D surface of vertical land movements (Fig. 8). It can be noticed that Port Said, Kafr El-Zaiat, and Tanta cities suffer from high land

subsidence rates ranging between 4.0 and 5.5 mm/year. On the other hand, Cairo, Belbis, Fakous and Burrllus cities subjected to a high trend of uplift within 3.1-4.7 mm/year. Such findings should be highly considered in the development plans of those cities, particularly for huge infrastructures.

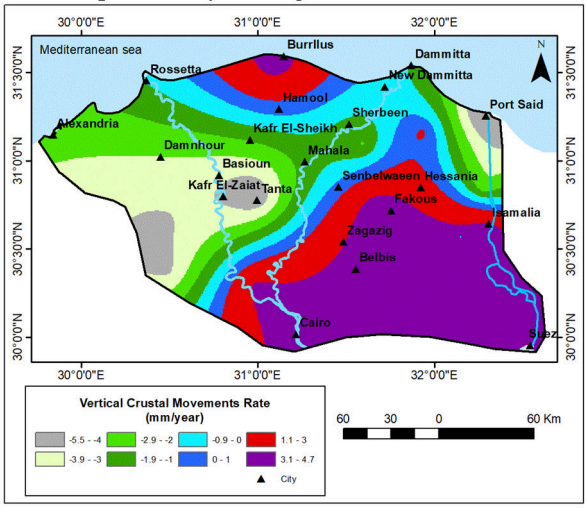

Figure 8: Vertical Land Movements in the Nile Delta at Main Cities

Finally, the effect of vertical land movements on Sea Level Rise (SLR) has been investigated too. It is worth mentioning that SLR observed at Tide Gauge (TG) is relative and the absolute SLR has to account for land subsidence at TG locations. Recent estimates of relative SLR at the Nile delta from two TG stations reveal that its annual rates equal 3.5 and 1.9 mm/year at Alexandria and Port Said respectively [23]. Regarding the accomplished results of vertical land movements in the Nile delta, it can be estimated that the absolute SRL rate at Alexandria and Port Said equal 6.0 and 7.6 mm/year respectively. Such imperative findings should be considered in any existing and upcoming development plans of the Nile Delta region.

Conclusions

Vertical land movements have major risky impacts from economic, environmental, and social perspectives. GNSS technologies have been commonly applied as a fundamental technical tool for monitoring horizontal and vertical land movements. In Egypt, several studies have been carried out for observing land subsidence as a hazardous phenomenon, particularly in the Nile delta region. The current research utilizes 24-hour GNSS datasets for 23 stations to observe vertical land motion over the period 2012-2019.

The variations of height, at each station, have been investigated and a linear regression model has been performed. Based on the available datasets, the coefficient of determination of the regression is found to be less than 0.20 over 7 stations which conclude that the linear regression model does not reflect the height variations at those stations. In addition, it has been realized that four stations have only 3 available observations (GNSS raw data) which means that the degree of freedom, in the regression modelling, just equals one. Accordingly, the reliability of the attained regression equations, at these stations, could not be considered confidential and those 11 stations have been neglected. Thus, the accomplished findings showed that the vertical land movements within the study area range from subsidence equals -5.5 mm/year to uplift equals 4.2 mm/year, with an overall average of -0.08 mm/year. Such land subsidence rates are very close to the results of other studies in the Nile delta region utilizing other techniques and datasets.

Recommendations

Few recommendations could be drawn, based on the achieved outcomes, for future works such as:

1. It is recommended that the accomplished results should be taken into account by decision makers in any existing and upcoming development plans of the Nile Delta resources management, particularly for water resources huge structures design such as barrages, weirs, and even canals or drains.
2. It is a matter of reality that vertical land motion is quite a vital phenomenon to be continuously monitored and analyzed particularly in low-land river deltas.
3. The current research recommends the continuation of GNSS-based monitoring of such phenomena over a longer time.

4. Furthermore, it is highly recommended to carry out comprehensive investigations for the natural, human, and geological factors affecting the land subsidence in the Nile delta area.

References

[1]. Othman, A. and Aboutalib, A. (2019). Land subsidence triggered by groundwater withdraw under hyper-arid conditions: case study from central Saudi Arabia, *Environmental Earth Sciences*, 78:243, https://doi.org/10.10007/s12665-019-8254-8.

[2]. Mohamed, H. (2015a). Assessment of factors influencing static GNSS precise point positioning: A case study in Egypt, *International Journal of Applied Sciences and Engineering Research*, 4(5):692-701.

[3]. Bozzano, F., Esposito, C., Franchi, S., Mazzanti, P., Perissin, D., Rocca, A., and Romano, E., (2015). Understanding the subsidence process of a quaternary plain by combining geological and hydrogeological modelling with satellite InSAR data: The Acque Albule Plain case study, *Remote Sensing of Environment*, (168):219–238.

[4]. Letetrel, C. Karpytchev, M., Bouin, M-N., Marcos, M., SantamarÍa-Gómez, A., and Wöppelmann, G. (2015). Estimation of vertical land movement rates along the coasts of the Gulf of Mexico over the past decades, *Continental Shelf Research*, (111):42–51.

[5]. Psimoulis, P., Ghilardi, M., Fouache, E., and Stiros, S. (2007). Subsidence and evolution of the Thessaloniki plain, Greece, based on historical leveling and GPS data, *Engineering Geology*, (90):55–70.

[6]. Yuwono, B., Awaluddin, M., Kun, F. and Lutfi, E. (2017). Evaluation of base station CORS UDIP and CSEM for monitoring ground deformation Sayung Demak Indonesia, The 5th Geoinformation Science Symposium 2017, https://doi.org/10.1088/1755-1315/98/1/012047.

[7]. Caló, F., Notti, D., Galve, J., Abdikan, S., Görüm, T., Pepe, A, and Sanli, F. (2017). DInSAR-Based detection of land subsidence and correlation with groundwater depletion in Konya plain, Turkey, *Journal of Remote Sensing*, (9), https://doi.org/10.3390/rs9010083.

[8]. Lamich, D., Marschalko, M., Yilmaz, I., Bednarova, P., Niemiec, D., Kubecka, K., and Mikulenka, V. (2015). Subsidence measurements in roads and implementation in land use plan optimization in areas affected by deep coal mining, *Journal of Environ Earth Science*, 75(69), https://doi.otg/10.1007/s12665-015-4933-2.

[9]. Frihy, O. (2017). Evaluation of future land-use planning initiatives to shoreline stability of Egypt's northern Nile delta, *Arabian Journal Geosciences*, https://doi.otg/10.1007/s12517-017-2893-4.

[10]. Stanley, J. and Clemente, P. (2017). Increased land subsidence and sea-level rise are submerging Egypt's Nile delta coastal margin, *The Geographical Society of America: GSA Today*, 27(5): 4-11.

[11]. AbouAly, N., Hussien, M., Rabah. M., Zidan, Z., and Saleh, M. (2021a). Land deformation monitoring by GNSS in the Nile delta and the measurements analysis, *Arabian Journal of Geosciences*, 14:150, https://doi.otg/10.1007/s12517-021-06497-6.

[12]. Rateb, A. and Abotalib, A. (2020). Inferencing the land subsidence in the Nile delta using Sentinel-A satellites and GPS between 2015 and 2019, *Science of the Total Environment*, https://doi.otg/10.1016/j.scitotenv.2020.138868.

[13]. Saleh, M. and Becker, M. (2019). New estimation of Nile delta subsidence rates from InSAR and GPS analysis, *Environmental Earth Science*, 78:6, https://doi.otg/10.1007/s12665-018-800-6.

[14]. Higgins, S. (2015). Review: Advances in delta-subsidence research using satellite methods, *Hydrogeological Journal*, https://doi.org/10.1007/s10040-015-1330-6.

[15]. AbouAly, N., Elhussien, M., Rabah. M., and Zidan, Z. (2021b). Assessment of NRCAN PPP on;ine service in determination of crustal velocity: case study northern Egypt GNSS network, *Arabian Journal of Geosciences*, 14:188, https://doi.otg/10.1007/s12517-021-06530-8.

[16]. Rabah, M., Elmewafey, M. and Farahan, M. (2016). Datum maintenance of the main Egyptian geodetic control networks by utilizing Precise Point Positioning (PPP) technique, *NRIAG Journal of Astronomy and Geophysics*, (5):96-105.

[17]. Abdallah, A., Agag, T. and Dawod, G. (2021). ITRF-based tectonic coordinates changes using GNSS-CORS network: A case study of Egypt, *Surveying and Land Information Science*, 80(2):69-78.

[18]. Zaid, S., Mamoun, M., and Al-Mobark, N. (2014). Vulnerability assessment of the impact of sea level rise and land subsidence on north Nile Delta region, *World Applied Sciences Journal*, 32(3):325-342.

[19]. SRI (Survey Research Institute) (2022). *Assessing and modelling of land subsidence in the Nile delta area and its effect on water structures, canals and drains*, Internal Technical Report, Giza, Egypt.

[20]. Hofmann-Wellenhof, B., Lichtenegger, H. and Wasle, E. (2007). *GNSS: Global Navigation Satellite Systems GPS, GLONASS, Galileo, and more*, Springer, New York, USA.
[21]. Mohamed, H., Shaheen, B., Hosney, M., and Dawod, G. (2015b). High-precision GPS monitoring of the land subsidence in the Nile Delta: Status and preliminary results, *Regional Conference on Surveying and Development*, Sharm El-Sheikh, Egypt, Oct. 3-6.
[22]. Abd Rabbou, M., El-Shazly, A., and Ahmed, K. (2017). Comparative analysis of multi-constellation GNSS single-frequency precise point positioning, *Survey Review*, https://doi.otg/10.1080/00396265.2017.1296628.
[23]. Dawod, G., Ebaid, H., Haggag, G. and Al-Krargy, E. (2021). An integrated geomatics approach for projecting sea level variations and risks: A case study in the Nile Delta, Egypt, *Journal of Architecture and Civil Engineering*, 6(8):24-38.